Journal of Petroleum Exploration and Production Technology (2023) 13:101–110
https://doi.org/10.1007/s13202-022-01538-6

ORIGINAL PAPER-PRODUCTION ENGINEERING

A new water flooding characteristic curve at ultra-high water cut stage

Shanshan Li[1] · Qihong Feng[1] · Xianmin Zhang[1] · Chunlei Yu[2] · Yingsong Huang[2]

Received: 19 January 2022 / Accepted: 13 June 2022 / Published online: 11 July 2022

Abstract
A large number of field practices show that the water flooding characteristic curve will appear up-warping phenomenon in ultra-high water cut stage, and the conventional water flooding characteristic curve is difficult to accurately characterize. In this work, a new expression of oil–water relative permeability ratio (K_{ro}/K_{rw}) and water saturation (S_w) is proposed based on the statistical analysis of experimental data of oil–water relative permeability at high displacement multiples. The new expression has a simpler form and fewer unknown parameters. The results show that the expression can accurately fit the later section of the conventional relative permeability ratio curve, and the correlation coefficient is above 0.996. On this basis, a new type of water flooding characteristic curve suitable for the whole process of water flooding reservoir development is established by combining the reservoir engineering method. Numerical simulation and field application show that the new curve has higher accuracy and wider applicability than conventional curve. The prediction error of recoverable reserves calculated by the new curve is only 0.22%, and the error of geological reserves is less than 5%. According to the comparison between the actual data and the predicted data, the actual cumulative oil production is 2.579×10^6 t, the predicted by the new curve is 2.569×10^6 t, the actual ultimate oil recovery is 50.235%, and the predicted is 50.04%. The predicted value is consistent with the actual one. It provides a more reliable method to accurately predict reservoir development indexes and guides the oilfield's subsequent decision-making.

Keywords Water flooding characteristic curve · Ultra-high water cut stage · High displacement · Oil–water relative permeability ratio · Performance prediction

List of Symbols

a	The fitting parameter
b	The fitting parameter
c	The fitting parameter
A	The fitting parameter
B	The fitting parameter
C	The fitting parameter
Q_o	Oil production, t d^{-1}
Q_w	Water production, t d^{-1}
μ_o	Oil viscosity, mPa s
μ_w	Water viscosity, mPa s
γ_o	Oil relative density
γ_w	Water relative density
K_{ro}	Oil-phase relative permeability
K_{rw}	Water-phase relative permeability
S_w	Water saturation
S_{or}	Residual oil saturation
B_o	Oil formation volume factor, m^3/m^3
B_w	Water formation volume factor, m^3/m^3
S_{wc}	Irreducible water saturation
WOR	Water–oil ratio
N_p	The cumulative oil production, 10^4 t
N	Geological reserves, 10^4 t
R	Oil recovery
f_w	Water cut

✉ Xianmin Zhang
Spemin@126.com

[1] School of Petroleum Engineering, China University of Petroleum (East China), Qingdao City 266580, Shandong Province, China

[2] Exploration and Development Research Institute, Shengli Oilfield Company, SINOPEC, Dongying City 257015, Shandong Province, China

Introduction

The water flooding characteristic curve has been widely used in water flooding oilfields, which can be used to predict the geological reserves, recoverable reserves and oil recovery of the oilfield, as well as future production performance

of the oilfield (Zhifang et al. 1990; Chen 2002; Ke and Jianwen 2013; Yuanqian and Weirui 2014; Wenjun 2020). The theoretical basis of traditional water flooding characteristic curve derivation is the semi-log linear relationship between oil–water relative permeability ratio (K_{ro}/K_{rw}) and water saturation (S_w) (Craft and Hawkins 1959; Wenjun and Zhengke 2000; Goda et al. 2007; Roghanian and Reza 2012; Can and Kabir 2014; Cuo and Chengfang 2017; Wenjun 2020; Li et al. 2021). However, with the continuous development of water flooding, when the reservoir enters the ultra-high water cut stage, the semi-log relationship between oil–water relative permeability ratio and water saturation is no longer completely linear, and the curve will bend downward (Bondar and Blasingame 2002; Jian 2013; Zhaojie and Fengpeng 2013; Chunlei 2014; Cao et al. 2021). Besides, a large number of oilfield practices have shown that the water flooding characteristic curve will also occur upward warping (Zhaojie and Fengpeng 2013; Baohong 2015; Chuanzhi and Duanping 2015; Cuo 2017; Hongen and Sibo 2019; Qi et al. 2022), which results in the application of conventional water flooding characteristic curve to predict the development indexes will have a non-negligible error.

Based on the phenomenon, some experts derived the water flooding characteristic curve suitable for the ultra-high water cut stage by the method of reverse or fractal theory (Guan and Wen-rui 2019; Andersen et al. 2020; Wenjun 2020; Liu et al. 2021). And most scholars proposed some special mathematical expression forms based on the conventional water flooding characteristic curve expression, such as polynomial function term (Zhaojie and Fengpeng 2013; Feng et al. 2014; Xiaolin and Zhiping 2015; Zhinbin 2015) or exponential function term (Dekang 2017; Jianwei and Yigen 2020). The water flooding characteristic curve generated in these ways will cause the left and right ends of the expression to be unequal when the water saturation approaches the extreme value. In addition, some experts have appended some special mathematical functions to the B-type water flooding characteristic curve, such as logarithmic function term (Chuanzhi and Duanping 2015; Zhinbin 2015; Zhibin 2016; Jiqiang and Shuhong 2017), trigonometric function form (Wang et al. 2013; Ke and Jinqing 2019) and infinite term rational polynomial form (Haohan 2019). Although the problem that the left and right ends of the expression are not equal has been solved, the "upward warping" phenomenon of the water flooding characteristic curve in ultra-high water cut stage cannot be accurately characterized. Meanwhile, there are also problems of complex relationship representation, low fitting accuracy and large prediction error.

In this study, through statistical analysis of the relative permeability experimental data of high displacement multiples, a new characterization formula describing the relationship curve of oil–water relative permeability ratio is proposed on the basis of the semi-log linear relationship between K_{ro}/K_{rw} and S_w. On this basis, a new water flooding characteristic curve is also established combined with the reservoir engineering method, which has the advantages of simple expression form and high fitting accuracy. Through the verification analysis and field application, the new curve can be used to accurately predict the development index of the ultra-high water cut reservoir and is suitable for the whole water flooding development process.

Besides, this work is organized as follows. In Sect. 2.1, a new model to characterize the relationship between K_{ro}/K_{rw} and S_w is proposed based on statistical experimental results, and then, according to the actual oilfield data, the new model is verified and compared with the traditional models (Sect. 2.2). In addition, based on reservoir engineering methods, a new water flooding characteristic curve is proposed (Sect. 3.1), and the new curve is justified by the numerical simulation result (Sect. 3.2). Field application of the type curve is presented in Sect. 4. In Sect. 5, we provide some concluding remarks.

Modification of seepage characteristic expression

Relative permeability characterization

At present, the expression commonly used to describe the quantitative relationship between oil–water relative permeability ratio and water saturation is (Craft and Hawkins 1959; Chen 2002) as follow:

$$\ln\left(K_{ro}/K_{rw}\right) = a + bS_w \tag{1}$$

where K_{ro} and K_{rw} are the oil phase relative permeability and the water phase relative permeability, respectively; S_w is the water saturation; a and b are the fitting parameters.

Equation (1) shows that oil–water relative permeability ratio (K_{ro}/K_{rw}) and water saturation (S_w) have a linear relationship under the semi-log coordinate. Yu et al. (Chunlei 2014; Baohong 2015) carried out relative permeability experiments with high displacement multiple. The relative permeability experiment is improved, and 124 sets of core tests with injection volume up to 1000 PV are carried out.

The $\mathbf{ln}(K_{ro}/K_{rw}) \sim S_w$ and $\mathrm{d}\mathbf{ln}(K_{ro}/K_{rw})/\mathrm{d}S_w \sim S_w$ variation of one core is presented in Fig. 1. The experiment showed that the worse the flow capacity of crude oil, the smaller the ratio of oil–water relative permeability, and the change rate is getting faster and faster at the ultra-high water cut stage. When exceeding the changing trend described by the logarithmic function, the curve of $\mathbf{ln}(K_{ro}/K_{rw}) \sim S_w$ will bend downward (see Fig. 1).

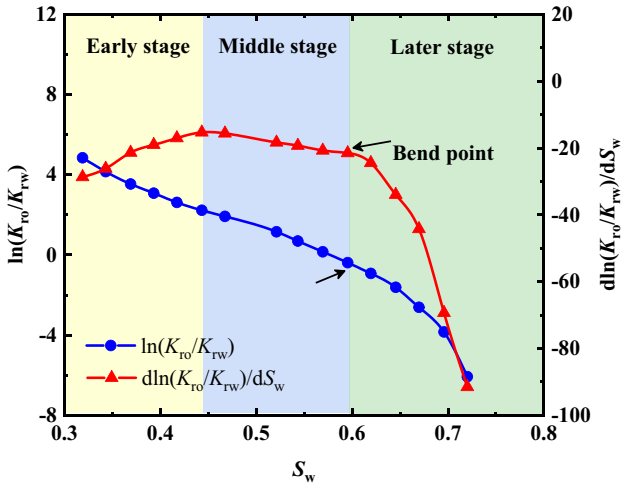

Fig. 1 Yu experiment of relative permeability ratio and slope change curve

Therefore, Eq. (1) can only describe the straight section at the middle stage of water flooding development, but cannot describe the downward curve section at the ultra-high water cut stage.

Through analyzing the oil–water relative permeability experiment data under high displacement multiples (Chunlei.Yu 2014), a new characterization relation between oil–water relative permeability ratio and water saturation is proposed based on Eq. (1):

$$\ln(K_{ro}/K_{rw}) = a + bS_w + 2\ln(c - S_w) \tag{2}$$

where c is the fitting parameter; a, b, and c can be estimated from a nonlinear least-square fit to the measured relative permeability data.

According to relative permeability experiments (Chunlei 2014), 11 groups of oil–water relative permeability ratio curves are chosen to be fitted by Eq. (2), and the fitting relationship between K_{ro}/K_{rw} and S_w is shown in Table 1. Meanwhile, residual oil saturation values of these rock samples measured experimentally are also given in Table 1.

As can be seen from Table 1, the new characterization (Eq. (2)) is used to fit the oil–water relative permeability ratio and water saturation. The fitting accuracy is extremely high, and the average correlation coefficient R^2 is more than 0.996.

Furthermore, the residual oil saturation S_{or} measured in 124 experiments and the parameter c obtained by fitting the relative permeability curve are summarized, and the relationship between c and 1-S_{or} is shown in Fig. 2.

It can be seen from Fig. 2 that each scatter point is distributed near the 45 line, which indicates that the difference between c and 1-S_{or} is very small. Therefore, when the residual oil saturation S_{or} is known, the fitting parameter c can be replaced by 1-S_{or}. Therefore, Eq. (2) can be further expressed as:

$$\ln(K_{ro}/K_{rw}) = a + bS_w + 2\ln(1 - S_{or} - S_w) \tag{3}$$

where S_{or} is the residual oil saturation.

Compared with Eq. (1), a logarithmic function term of 1-S_{or}-S_w is added to Eq. (3), which can increase the fitting adaptability of the curve segment. The law reflected by Eq. (3) has obvious physical meaning in water flooding development. That is, when S_w infinitely approaches 1-S_{or}, K_{ro} will also approach 0, and then, $\ln(K_{ro}/K_{rw})$ will be close to $-\infty$, which is similar to the water flooding law consistency. Thus, Eq. (3) describes the relationship between K_{ro}/K_{rw} and S_w can be applied to the whole process of water flooding development.

Model verification

In order to further verify the general applicability and accuracy of Eq. (3), the typical $\ln(K_{ro}/K_{rw}) \sim S_w$ curves of four actual blocks(Jiqiang and Shuhong 2017) are selected and fitted by Eqs. (1), (3) and the expressions (Eq. 4) (Jian 2013;

Table 1 The fitting result table of relative permeability experimental data by Eq. (2)

Rock sample	Fitting relation	S_{or} experimental value	R^2
1	$\ln(K_{ro}/K_{rw}) = 9.8985 - 13.3007S_w + 2\ln(0.7288 - S_w)$	0.2815	0.9993
2	$\ln(K_{ro}/K_{rw}) = 10.3699 - 17.1878S_w + 2\ln(0.7046 - S_w)$	0.3001	0.9993
3	$\ln(K_{ro}/K_{rw}) = 8.6128 - 8.7640S_w + 2\ln(0.8417 - S_w)$	0.1655	0.9950
4	$\ln(K_{ro}/K_{rw}) = 7.0522 - 10.7520S_w + 2\ln(0.8461 - S_w)$	0.1799	0.9865
5	$\ln(K_{ro}/K_{rw}) = 7.2542 - 9.6618s_w + 2\ln(0.7284 - S_w)$	0.2766	0.9951
6	$\ln(K_{ro}/K_{rw}) = 17.2856 - 27.6813S_w + 2\ln(0.7065 - S_w)$	0.3248	0.9988
7	$\ln(K_{ro}/K_{rw}) = 10.8419 - 16.2243S_w + 2\ln(0.8123 - S_w)$	0.1588	0.9994
8	$\ln(K_{ro}/K_{rw}) = 10.9550 - 14.8285S_w + 2\ln(0.7718 - S_w)$	0.2537	0.9997
9	$\ln(K_{ro}/K_{rw}) = 6.1217 - 5.1425S_w + 2\ln(0.8012 - S_w)$	0.2208	0.9995
10	$\ln(K_{ro}/K_{rw}) = 9.7589 - 13.5052S_w + 2\ln(0.7504 - S_w)$	0.2495	0.9994
11	$\ln(K_{ro}/K_{rw}) = 11.0339 - 14.4960S_w + 2\ln(0.8437 - S_w)$	0.1301	0.9854

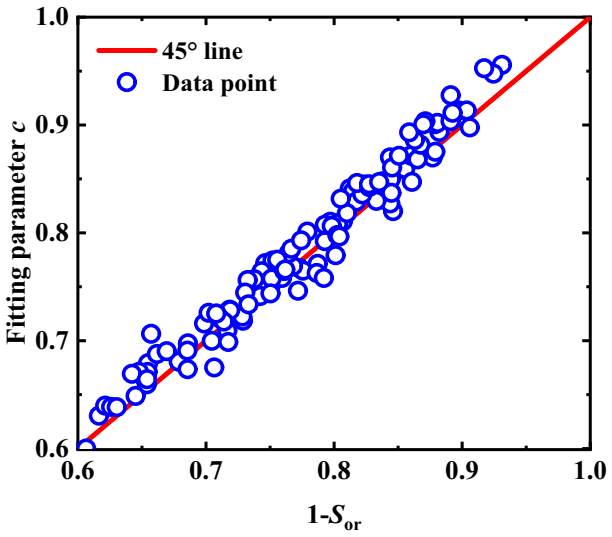

Fig. 2 Plot of the fitting parameter c vs. 1-S_{or}

Jiqiang and Shuhong 2017), respectively. The fitting results are shown in Figs. 3 and 4.

$$\ln(K_{ro}/K_{rw}) = a + bS_w + ce^{S_w} \tag{4}$$

It can be seen from Figs. 3 and 4 that the new expression Eq. (3) has the highest fitting accuracy, followed by Eq. (4) and Eq. (1). Among them, Eq. (1) is a linear equation, which has the worst adaptability to the curved line segments at the ultra-high water cut stage. In addition, although Eq. (4) can describe the downward curve to a certain extent, the fitting accuracy is significantly lower than that of Eq. (3). Besides, Eq. (4) is difficult to obtain the type-B characteristic curve through derivation. However, Eq. (3) is a simpler form and fewer unknown parameters, which can well characterize the relationship between K_{ro}/K_{rw} and S_w in the whole process of water flooding development.

New type water flooding characteristic curve

Derivation of new type curve

The conventional B-type water flooding characteristic curve has universal applicability in water flooding development oilfields, and its expression is:

$$\ln WOR = a + bN_p \tag{5}$$

where WOR is water–oil ratio; N_p is the cumulative oil production, 10^4 t.

Equation (5) shows a linear relationship between water–oil ratio (WOR) and cumulative oil production (N_p) under the semi-log coordinate. The method of linear segment extrapolation can be used to determine the ultimate recovery and recoverable reserves (Shuhua 2001). However, during actual oilfield production and laboratory tests, it was found that the B-type water flooding characteristic curve is no longer applicable at the ultra-high water-cut stage, and the curve of this stage will be up-warping.

In order to accurately describe the up-warping phenomenon, a new water flooding characteristic curve is established on the above expression Eq. (2) or Eq. (3) and combined with the reservoir engineering method.

In the stable seepage condition of water flooding, regardless of the gravity and capillary force influence, the relationship between the oil–water relative permeability ratio and oil–water production is as follows (Hanqiao et al. 2006):

$$\frac{K_{ro}}{K_{rw}} = \frac{Q_o\mu_o B_o\gamma_w}{Q_w\mu_w B_w\gamma_o} \tag{6}$$

where Q_o and Q_w are the output of surface crude oil and surface water, respectively, t·d^{-1}; μ_o and μ_w are the viscosity of formation crude oil and formation water, respectively, mPa·s; B_o and B_w are, respectively, the volume coefficients of formation crude oil and formation water, without dimensionality; γ_o and γ_w are the relative density of surface degassed crude oil and surface water, without dimensionality.

Equation (2) can be transformed into the following form:

$$\frac{K_{ro}}{K_{rw}} = (c - S_w)^2 e^{a+bS_w} \tag{7}$$

Combining Eqs. (6) and (7), we can get:

$$WOR = \frac{Q_o}{Q_w} = \frac{\mu_o B_o\gamma_w}{\mu_w B_w\gamma_o}(c - S_w)^{-2}e^{-(a+bS_w)} \tag{8}$$

Besides, water saturation can be expressed as (Buckley and Leverett 1942):

$$S_w = \frac{1 - S_{wc}}{N}N_p + S_{wc} = 1 - (1 - R)(1 - S_{wc}) \tag{9}$$

where S_{wc} is irreducible water saturation; N_p is the cumulative oil production, 10^4 t; N is geological reserves, 10^4 t, R is oil recovery:

$$R = \frac{N_p}{N} \tag{10}$$

Substitute Eq. (9) into Eq. (8) and take the logarithm of both sides to obtain that:

$$\begin{aligned}\ln WOR = \ln\frac{\mu_o B_o\gamma_w}{\mu_w B_w\gamma_o} - 2\ln\left[c - 1 + (1 - R)(1 - S_{wc})\right] \\ +b(1 - R)(1 - S_{wc}) - a - b\end{aligned} \tag{11}$$

Then, substituting Eq. (10) into Eq. (11) and sorting $\ln WOR$ out, it can be obtained:

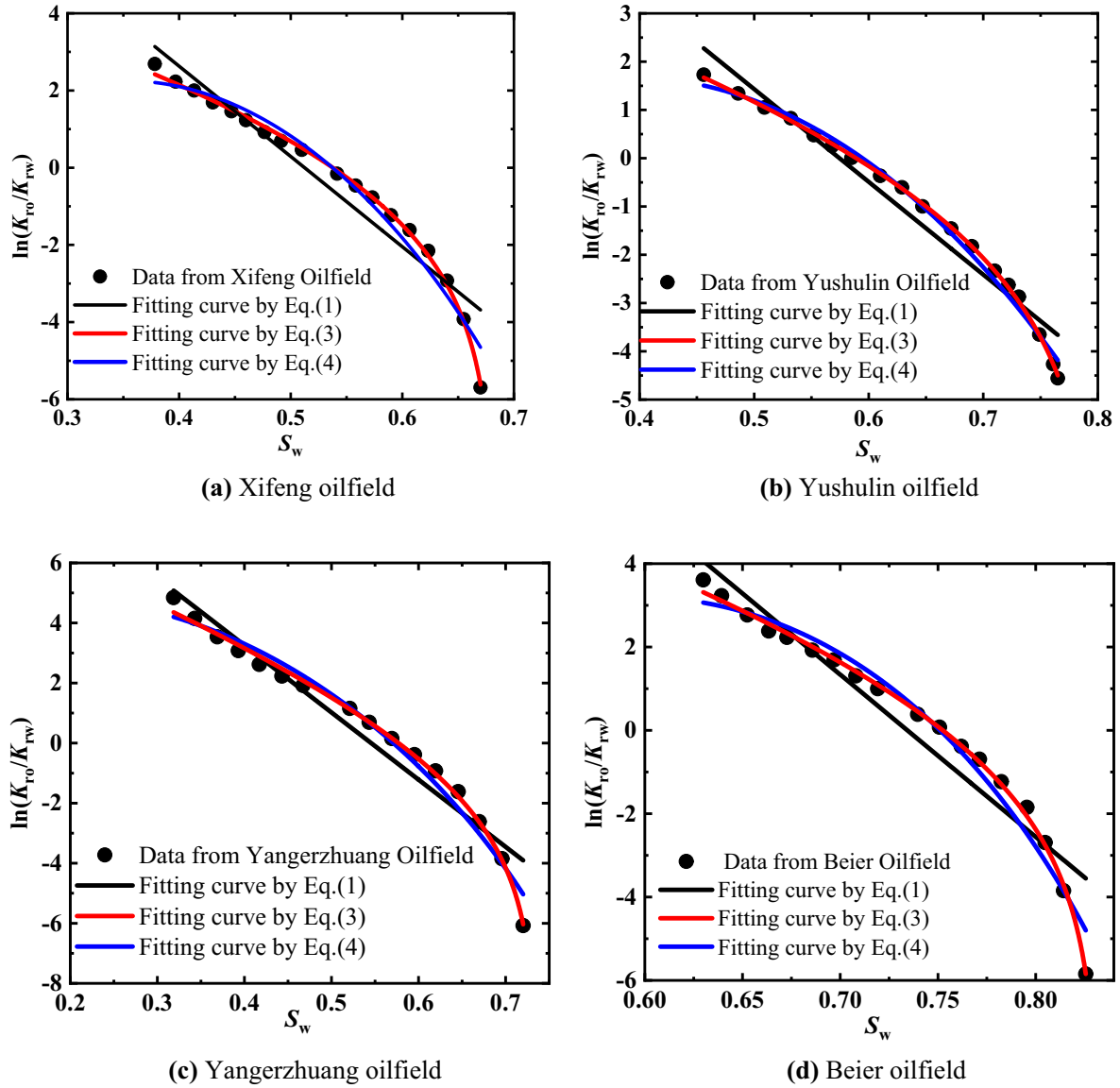

Fig. 3 Fitting results of four oilfields by Eqs. (1), (3), and (4)

$$
\begin{aligned}
\ln WOR &= \ln\frac{\mu_o B_o \gamma_w}{\mu_w B_w \gamma_o} - 2\ln\left[c - 1 + (1 - \frac{N_p}{N})(1 - S_{wc})\right] + b(1 - \frac{N_p}{N})(1 - S_{wc}) - a - b \\
&= \ln\frac{\mu_o B_o \gamma_w}{\mu_w B_w \gamma_o} - 2\ln\left[\frac{(c-1)N + (N - N_p)(1 - S_{wc})}{N}\right] + \frac{b(N - N_p)(1 - S_{wc}) - bN}{N} - a \\
&= \ln\frac{\mu_o B_o \gamma_w}{\mu_w B_w \gamma_o} - 2\ln\left[\frac{(c - S_{wc})N - (1 - S_{wc})N_p}{N}\right] - \frac{bNS_{wc} + bN_p(1 - S_{wc})}{N} - a \\
&= \ln\frac{\mu_o B_o \gamma_w}{\mu_w B_w \gamma_o} - 2\ln\left[\frac{(c - S_{wc})N - (1 - S_{wc})N_p}{N}\frac{N}{1 - S_{wc}} \Big/ \frac{N}{1 - S_{wc}}\right] - b\frac{1 - S_{wc}}{N}N_p \\
&\quad - bS_{wc} - a \\
&= -b\frac{1 - S_{wc}}{N}N_p - 2\ln\left(N\frac{c - S_{wc}}{1 - S_{wc}} - N_p\right) + \ln\frac{\mu_o B_o \gamma_w}{\mu_w B_w \gamma_o} + 2\ln\frac{N}{1 - S_{wc}} - bS_{wc} - a
\end{aligned}
\tag{12}
$$

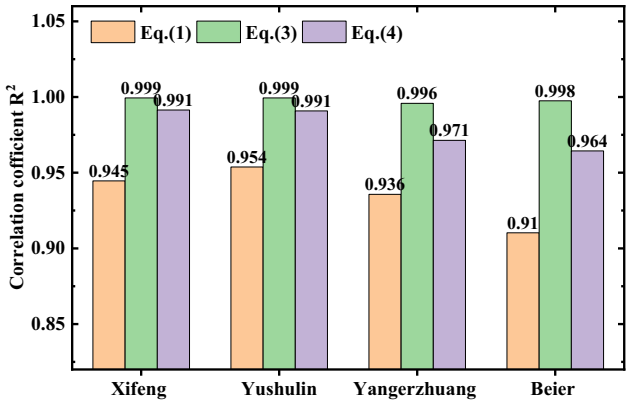

Fig. 4 The correlation coefficients of the four oilfields, respectively, by using Eqs. (1), (3), and (4)

Let:

$$A = \ln\frac{\mu_o B_o \gamma_w}{\mu_w B_w \gamma_o} + 2\ln\frac{N}{1 - S_{\mathrm{wc}}} - bS_{\mathrm{wc}} - a \tag{13}$$

$$B = b\frac{1 - S_{\mathrm{wc}}}{N} \tag{14}$$

$$C = N\frac{c - S_{\mathrm{wc}}}{1 - S_{\mathrm{wc}}} \tag{15}$$

where A, B, C are the fitting parameters, respectively.

The expression of the new water flooding characteristic curve can be obtained as:

$$\mathbf{ln}WOR = A - BN_{\mathrm{p}} - 2\mathbf{ln}\left(C - N_{\mathrm{p}}\right) \tag{16}$$

According to definitions of $WOR = \frac{Q_{\mathrm{o}}}{Q_{\mathrm{w}}}$ and $f_{\mathrm{w}} = \frac{Q_{\mathrm{w}}}{Q_{\mathrm{o}}+Q_{\mathrm{w}}}$, we can get that:

$$WOR = \frac{f_{\mathrm{w}}}{1 - f_{\mathrm{w}}} \tag{17}$$

where f_{w} is water cut.

Substituting Eq. (17) into Eqs. (16), (16) can also be expressed as:

$$\mathbf{ln}\frac{f_{\mathrm{w}}}{1 - f_{\mathrm{w}}} = A - BN_{\mathrm{p}} - 2\mathbf{ln}(C - N_{\mathrm{p}}) \tag{18}$$

Equation (16) is the new type of water flooding characteristic curve equation, which reflects the relationship between water–oil ratio (WOR) and cumulative oil production (N_{p}) at the later stage of water flooding development, so it is suitable for the ultra-high water-cut stage.

As the oil recovery (R) is low, the cumulative oil production (N_{p}) will also be very low, that is, $\mathbf{ln}(C\text{-}N_{\mathrm{p}})$ tends to 0. In this case, Eq. (16) can be written as $\mathbf{ln}WOR = A\text{-}BN_{\mathrm{p}}$, which is the familiar Eq. (6) of B-type water flooding characteristic curve. Therefore, the B-type water flooding characteristic curve is a special case of the new type water flooding characteristic curve when the oil recovery is low.

Besides, when the oilfield development reaches the economic limit water–oil ratio (In general, water–oil ratio is 49 or water cut is 98%) under the abandonment condition, the recoverable reserves and oil recovery can be predicted by Eq. (16) or Eq. (18). Furthermore, Eq. (16) can also be used to predict the future development of the oilfield and calculate the geological reserves of the oilfield.

Model verification

In order to verify the accuracy and applicability of the new water flooding characteristic curve, a five-spot well pattern model is established on the actual reservoir geological characteristics. The traditional type curve (Eq. (5)) and the new water flooding characteristic curve (Eq. 16) are used to fit the production performance, respectively.

The grid number of the model is $49 \times 49 \times 4$, the grid length is 15 m, the vertical grid length is 8 m, and the balance between injection and production. The basic parameters are presented in Table 2, and the relative permeability of oil and water is shown in Fig. 5.

Basis on numerical simulation results, the new water flooding characteristic curve is applied and compared with the conventional B-type water flooding characteristic curve. In the case of known residual oil saturation, data in Fig. 5 are fitted based on the new oil–water relative permeability ratio characterization Eq. (3), and fitting parameters in Eq. (3) are obtained as follows: $a = 6.1802$, $b = -5.2134$.

The calculation results of N_{p} and $\mathbf{ln}WOR$ are fitted by Eqs. (5) and (16), and the fitting results are shown in Fig. 6 and Table 3.

It can be seen from Fig. 6 and Table 3 that the conventional B-type water flooding characteristic curve can only fit the straight line segment at the early stage, and the upwarping curve segment in the later period could not be fitted effectively. However, the application of the new curve can realize the high precision fitting of the whole water flooding development process, and the fitting correlation coefficient is more than 0.9993.

By extrapolating to the limit water–oil ratio ($WOR = 49$) by the B-type water flooding characteristic curve, the calculated recoverable reserves of the reservoir are 33.9521×10^4 t, which has an error of more than 20% compared with the actual recoverable reserves of 27.0513×10^4 t (see Figs. 6, 7). However, the calculated recoverable reserves by the new curve are 27.1101×10^4 t, and the prediction error is only 0.22%.

Table 2 Basic parameters of the simulation case

Parameters	Value
Average porosity (%)	23.2
Permeability (10^{-3} μm^2)	123.79
Oil density (g/cm^3)	0.815
Irreducible water saturation	0.316
Residual oil saturation	0.202
Oil–water viscosity ratio	100
Geological reserves (10^4t)	210.6459

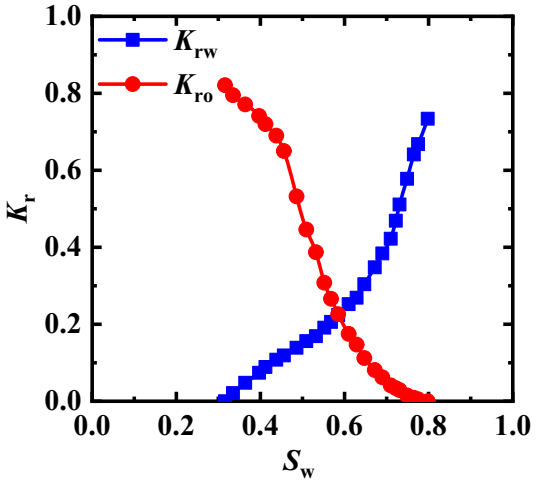

Fig. 5 Oil–water relative permeability

Besides, it can be seen from Table 3 that the fitting parameters of the new water flooding characteristic curve are: $A=7.6860$, $B=$-0.0177, $C=35.5337$. Therefore, according to Eq. (14), the deduction can be obtained:

$$N = b\frac{1-S_{wc}}{B} \tag{19}$$

And then, the geological reserves of the reservoir can be obtained by substituting the above parameters into Eq. (19): $N=201.4670\times10^4$ t. Furthermore, compared with the actual geological reserves of 210.6459×10^4 t, the relative error between them is less than 5%. This shows the new water flooding characteristic curve has higher accuracy and wider applicability, and it is suitable for the whole process of water flooding development.

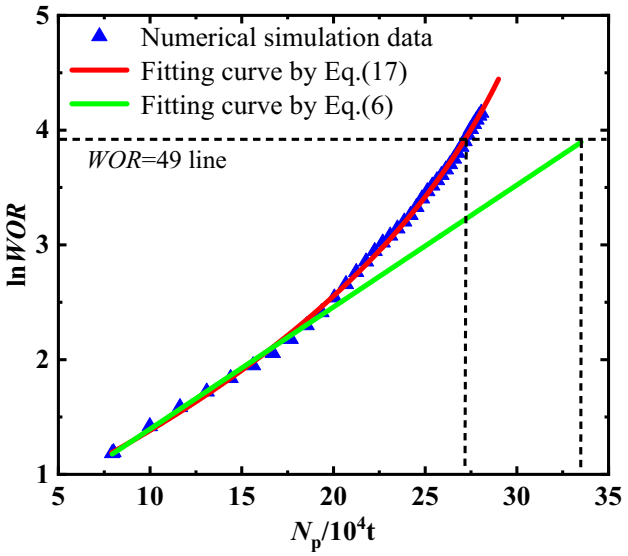

Fig. 6 Fitting result comparison of different water flooding characteristic curves

Table 3 Fitting expressions of different water flooding characteristic curves

Curve type	Fit relation	Correlation coefficient
B-type water flooding characteristic curve (Eq. 5)	$\ln WOR = 0.3323 + 0.1063N_p$	0.9121
New water flooding characteristic curve (Eq. 16)	$\ln WOR = 7.6860 + 0.0177N_p - 2\ln(35.5337 - N_p)$	0.9993

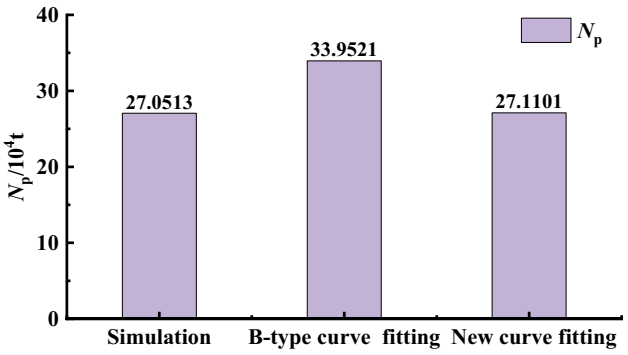

Fig. 7 Fitting results: comparison of different water drive characteristic curves and numerical simulation results ($WOR=49$)

Field application

The proposed type function has been employed in the northern part of west Gudao oilfield (GD oilfield), China.

The northern part of the west Gudao oilfield is located in the Neogene large draping belt in the east of Zhanhua sag, Jiyang depression, and it is a large drapery anticlinal integrated heavy oil reservoir with unconsolidated sandstone of Guantao Formation in tertiary. A set of thick oil reservoirs are developed in the upper Ng3 and lower Ng4 formations. The average thickness of sand bodies in $Ng3^5$ and $Ng4^4$ is 10–12 m, and the average effective thickness is 9 m. The target block has an oil-bearing area of 1.54 km^2, and the average porosity and permeability are 0.341 and 3213×10^{-3} μm^2, respectively, belonging to a medium–high permeability reservoir. The original oil in place of the reservoir is 5.1342×10^6 t. After normalizing the oil–water relative permeability curve (see Fig. 8), the irreducible water saturation is 0.319 and the residual oil saturation is 0.242.

The actual development data of the block are shown in Fig. 9. The reservoir was transferred to water flooding development after 2002, from 2002 to 2006, the comprehensive water cut of the reservoir was lower than 90%, and it was in the stage of medium–high water cut. While in 2010, the comprehensive water cut rose to 95% and the reservoir entered the ultra-high water cut stage. At present, the water cut of the reservoir has reached 98.924%, and the oil recovery is 50.235%.

According to the actual reservoir production data, the production data before the water cut of 95.156% (*WOR* is 19.644) are fitted by using the new water flooding characteristic curve (Eq. (16)) and Eq. (20) (Jian 2013, Jiqiang. Wang 2017) derived from formula (4), respectively, while the subsequent production data are used as the validation data of the prediction segment.

$$\ln WOR = a + bN_p + ce^{dN_p} \tag{20}$$

As shown in Fig. 10, the new water flooding characteristic curve (Eq. (16)) is used to fit the previous data, and the results show that the fitting accuracy is high, and the correlation coefficient is above 0.999. Equation (20) also has a good fitting effect on early stage production data. Besides, the relationship of the new water flooding characteristic curve of GD oilfield obtained by fitting is as follows:

$$\ln WOR = 1.6525 + 0.2977N_p - 2\ln(2.9183 - N_p) \tag{21}$$

In the prediction stage, the prediction results obtained by using Eq. (16) can coincide with the actual data. In addition, when the comprehensive water cut reaches 98.924% (the ultimate *WOR* is 92), the ultimate recoverable reserves predicted by Eq. (21) are 2.5691×10^6 t, and the corresponding ultimate oil recovery is 50.04%. The recoverable reserves and recovery calculated from the new model are very close to the actual values (the actual cumulative oil production is 2.579×10^6 t and the ultimate recovery is 50.235%), which

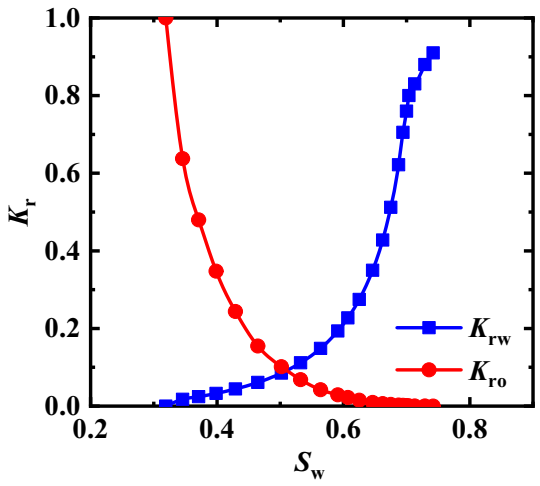

Fig. 8 Oil–water relative permeability of the target reservoir

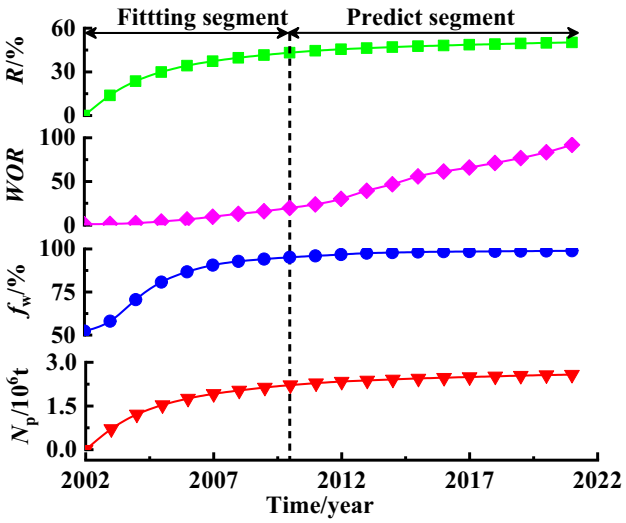

Fig. 9 The actual development data of the target reservoir

justifies the practical value of our model in actual oilfields (see Figs. 10, 11). However, the predicted results of Eq. (20) are quite different from the actual results.

Therefore, the new water flooding characteristic curve established in this paper can not only reflect the special oil–water seepage law in ultra-high water cut stage, but also has the advantages of simpler form and more accurate prediction results. It is suitable for the whole process of water flooding reservoir development and can provide a basis for oilfield development decision in high water cut stage.

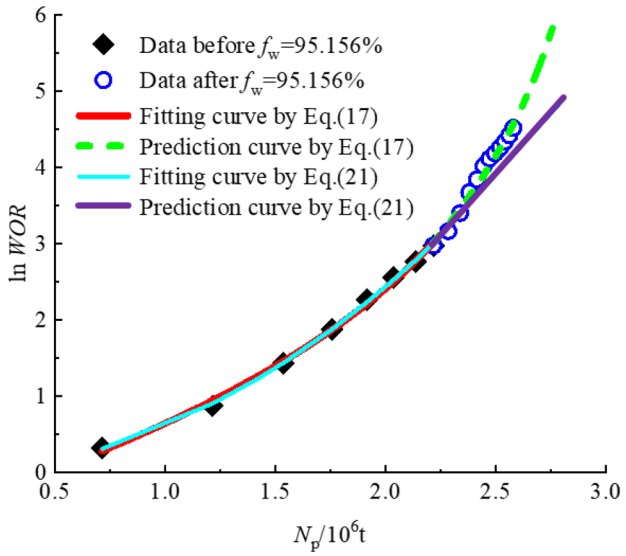

Fig. 10 Comparison of new water flooding characteristic curve (Eq. (16)) and existing one (Eq. (21)) in fitting and predicting development performance

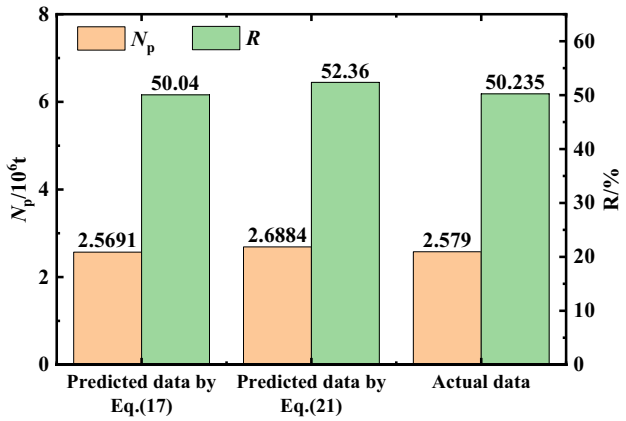

Fig. 11 Prediction results: new curve vs. existing curve in cumulative oil production and recovery (WOR = 92)

Conclusions

1) By statistical analysis of the experimental data of phase permeability with high displacement multiple, a new relationship between the ratio of oil–water relative permeability and water saturation is proposed. The expression is simple in form and has high fitting accuracy, which well solves the problem of characterizing the relationship between K_{ro}/K_{rw} and S_w in the whole process of water flooding development.
2) Based on the improved model, a new type of water flooding characteristic curve is derived and established. Compared with the conventional water flooding characteristic curve, the new curve has higher accuracy and wider applicability, which can achieve a high-precision fitting of the whole process of water flooding development. And the fitting correlation coefficient is more than 0.9993. The prediction error of recoverable reserves calculated by the new curve is only 0.22%, and the error of geological reserves is less than 5%. Besides, the curve can accurately predict the recoverable reserves and oil recovery of ultra-high water cut reservoirs, which provides a basis for oilfield development decisions in high water cut period.

Acknowledgements This research is supported by the National Science and Technology Major Project of China (Grant No.2016ZX05025001-006).

Funding National Science and Technology Major Project of China, Grant No. 2016ZX05025001-006, Qihong Feng.

Declarations

Conflict of interest The authors declare that they have no known competing financial interests or personal relationships that could have appeared to influence the work reported in this paper.

References

Andersen PØ et al (2020) simulation interpretation of capillary pressure and relative permeability from laboratory waterflooding experiments in preferentially oil-wet porous media. SPE Reserv Eval Eng 23(01):230–246. https://doi.org/10.2118/197065-PA

Baohong L (2015) A new method for judging the timing of the inflection point of the water drive characteristic curve in the ultra-high water cut period. Petrol Geol Recov Eff 22(05):103–106. https://doi.org/10.13673/j.cnki.cn37-1359/te.2015.05.016

Bondar V, Blasingame T (2002) Analysis and interpretation of water-oil-ratio performance. J Soc Petrol Eng

Buckley SE, Leverett MC (1942) Mechanism of fluid displacement in sands. Trans AIME 146(01):107–116. https://doi.org/10.2118/942107-G

Can B, Kabir CS (2014) Simple tools for forecasting waterflood performance. J Petrol Sci Eng 120:111–118. https://doi.org/10.1016/j.petrol.2014.05.028

Cao RY et al (2021) Displacement behavior and mechanism of long-term water flooding in sandstone oil reservoirs. J Central South Univ 28(3):834–847. https://doi.org/10.1007/s11771-021-4648-3

Chuanzhi CJX, Duanping W (2015) A new type of water drive characteristic curve in the ultra-high water cut stage. Acta Petrolei Sinica 36(10):1267–1271. https://doi.org/10.7623/syxb201510009

Chunlei Y (2014) A prediction method of phase permeability curve reflecting the limit of water drive. Special Oil and Gas Reserv 21(02):123–126. https://doi.org/10.3969/j.issn.1006-6535.2014.02.028

Craft B, Hawkins M (1959) Applied petroleum reservoir engineering. Prentice-Hall Inc, New Jersey

Cuo GYL, Chengfang S (2017) A new understanding of the up-warping of water flooding characteristic curve during ultra-high water cut period. Daqing Petrol Geol Develop 36(02):64–68. https://doi.org/10.3969/j.issn.1000-3754.2017.02.010

Dekang Z (2017) Modeling and application of multiple power exponential generalized water drive characteristic curve. Acta Petrolei Sinica 38(03):333–341. https://doi.org/10.7623/syxb201703010

Feng XLM, Xianghong W, Tianjian S, Yutao D, Xiao T, Rongrong J (2014) New expression of oil/water relative permeability ratio vs. water saturation and its application in water flooding curve. 32(5): 817–830.

Goda HM, et al (2007) of Conference. Use of artificial intelligence techniques for predicting irreducible water saturation—Australian hydrocarbon basins. All Days, Jakarta, Indonesia, Society of Petroleum Engineers. https://doi.org/10.2118/109886-ms

Guan CYL, Wen-rui HU (2019) A new type of water flooding characteristic curve based on fractal theory. J Math Practice Theory 49(09):124–129

Hanqiao J et al (2006) The fundamental and practice of reservoir engineering. China University of Petroleum Press, Dongying, pp 239–241

Haohan LYY (2019) New theory and practice of characterizing phase infiltration relationships in ultra-high water-cut period. J Southwest Petrol Univ (natural Sci Edition) 41(02):127–136. https://doi.org/10.11885/j.issn.1674-5086.2018.08.04.01

Hongen DHZ, Sibo S (2019) Correct understanding and application of waterflooding characteristic curve. Pet Explor Dev 46(04):755–762. https://doi.org/10.11698/PED.2019.04.14

Jian H (2013) Improvement of water displacement curve for water flooded oil reservoirs at ultra-high water cut stage. J China Univ Petrol (edition Natural Sci) 37(06):72–75. https://doi.org/10.3969/j.issn.1673-5005.2013.06.011

Jian HRW, Zhizeng X (2013) Improvement of type a waterflooding characteristic curve in ultra-high water cut period. J China Univ Petrol (natural Sci Edition) 37(06):72–75

Jianwei GYR, Yigen Z (2020) Research and application of an improved type B water drive characteristic curve. Special Oil Gas Reserv 27(01):102–107

Jiqiang WCS, Shuhong J (2017) New water drive characteristic curves at ultra-high water cut stage. Pet Explor Dev 44(06):955–960. https://doi.org/10.11698/PED.2017.06.13

Ke LSH, Jinqing Z (2019) A new type of water flooding characteristic curve and its application. Oil Gas Reserv Eval Develop 9(02):13–16+20

Ke ZHX, Jianwen C (2013) Discussion on the characteristic empirical formula of Tong's Type B water drive. J China Univ Petrol (edition Natural Sci) 37(01):99–103

Li C et al. (2021) A new measurement of anisotropic relative permeability and its application in numerical simulation. Energies 14(16):4731. https://doi.org/10.3390/en14164731

Liu Y et al (2021) Derivation of water flooding characteristic curve for offshore low-amplitude structural reservoir with strong bottom water. J Petrol Explor Prod Technol 11(8):3267–3276. https://doi.org/10.1007/s13202-021-01240-z

Qi G et al (2022) A new relative permeability characterization method considering high waterflooding pore volume. Energies 15(11): 3868. https://doi.org/10.3390/en15113868

Roghanian RRM, Reza HM (2012) Prediction of key points of water-oil relative permeability curves using the linear regression technique. Liq Fuel Technol 30(5):518–533

Shuhua WFY, Jiwei S (2001) Several problems that should be paid attention to when using water drive characteristic curve method to calculate recoverable reserves. Petrol Explor Develop (05): 53–55

Wang RR, Hou J, Li ZQ, Bing SX, Wu HJ, Wang H (2013) A new water displacement curve for the high water-cut stage. Pet Sci Technol 31(13):1327–1334. https://doi.org/10.1080/10916466.2012.756015

Wenjun GAOCP, Zhengke LI (2000). The theoretical basis and general method of seepage flow in deriving water drive characteristic curve. Petrol Explor Develop (05):56–60

Wenjun GRY, Jing Y (2020) Establishment and theoretical basis of a new type of water drive characteristic curve. Acta Petrolei Sinica 41(03):342–347

Wenjun GZL, Longlong X (2020) Determination of seepage equation of water drive characteristic curve by reverse derivation method. Fault Block Oil and Gas Field 27(04):478–483. https://doi.org/10.6056/dkyqt202004014

Xiaolin WLY, Zhiping L (2015) New water-flooding characteristic curves at the stage of extra-high water cut. Daqing Petrol Geol Develop 34(06):54–56. https://doi.org/10.3969/j.issn.1000-3754.2015.06.009

Chen Y (2002) Practical methods of oil and gas reservoir engineering. Petroleum Industry Press, Beijing

Yuanqian CEG, Weirui Z (2014) Question, comparison and review on "A kind of generalized water drive curve." Fault-Block Oil and Gas Field 21(02):205–207. https://doi.org/10.6056/dkyqt201402015

Zhaojie SZL, Fengpeng L (2013) Derivation of water flooding characteristic curve for high water-cut oilfields. Pet Explor Dev 40(02):201–208. https://doi.org/10.11698/PED.2013.02.09

Zhibin ZJW (2016) Research and application of a new type of water flooding characteristic curve in oilfield development. Adv Petrol Explor Develop 11(2):1–5

Zhifang L, Qitai YU, Wenxing LI (1990) A method for estimating recoverable reserves of an oil field by using the displacement characteristic curves. Petrol Explor Develop 17(6):64–71

Zhinbin LHL (2015) An effective method to predict oil recovery in high water cut stage. J Hydrodyn (6): 988–995. https://doi.org/10.1016/S1001-6058(15)60561-3.